 DOI: https://doi.org/10.5114/ceji.2022.115710

Scopoletin protects retinal ganglion cells 5 from high glucose-induced injury in a cellular model of diabetic retinopathy via ROS-dependent p38 and JNK signaling cascade

JINXIN PAN, HAOJIE LIU, QI WU, MING ZHOU

Department of Ophthalmology, Affiliated Zhongshan Hospital of Dalian University, Dalian, China

Abstract

The protective activity of scopoletin (SPT) against glucose-induced cataract has been attributed to attenuation of aldose reductase activity and oxidative stress in a rat model. The present investigation was aimed to study the protective effect and mechanism of SPT in retinal ganglia cells (RGC) under oxidative stress and apoptosis induced by hyperglycemia. The RGC-5 cells were pre-conditioned with variable SPT concentrations for 6 hours and then subjected to hyperglycemia for 48 hours. The cell viability, mitochondrial membrane potential (MMP) and oxidative stress markers were quantified. Western blotting was employed to screen the expression of mitogen-activated protein kinase (MAPK) and various apoptosis related proteins. SPT blocked the high-glucose induced cell injury and normalized the mitochondrial functioning via lowering the loss of MMP and release of cytochrome c. Pretreatment with SPT suppressed the enhanced ROS, malondialdehyde, and protein carbonyl content triggered by high-glucose exposure in RGC-5 cells. SPT normalized the apoptotic proteins in RGC-5 cells. The phosphorylation of c-Jun N-terminal kinases (JNK) and p38 MAPK in RGC-5 due to hyperglycemia was attenuated by SPT. Overall, SPT exhibited a protective effect in RGC-5 cells exposed to a high-glucose environment via its antioxidant efficacy, inhibition of apoptosis and modulation of the ROS-dependent p38/JNK signaling cascade.

Key words: *scopoletin, diabetic retinopathy, RGC-5, oxidative stress, reactive oxygen species.*

(Cent Eur J Immunol 2022; 47 (1): 20-29)

Introduction

Diabetic retinopathy (DR) is one of the foremost reasons for loss of sight and reversible blindness in individuals from 20 to 74 years, specifically in developing and developed nations [1]. Reports reveal that DR is more prevalent in people with type 1 diabetes compared to those with type 2 diabetes [2]. DR is associated with extended duration of diabetes and imbalanced glucose levels and blood pressure. DR, being a critical diabetic microvascular complication, is marked by gradual enhancement of vascular permeability, reduced blood perfusion to the retina and subsequent edema, leading to impairment of normal vision or blindness [3]. Previous investigations suggest that the primary indications of DR are correlated with loss of functionality and death of retinal ganglion cells (RGCs), which are the eccentric neurons designed to transfer the retinal perception to the visual center in the brain [4]. The vascular endothelial cells of the retina actively maintain the integrity of the blood-retinal barrier so that the retinal homeostasis is synchronized. Increased blood glucose levels may trigger oxidative stress and gives rise to reactive oxygen species (ROS), which eventually leads to structural and functional damage to the RGCs, thereby leading to defects in the normal vision and progressive blindness [5]. Further, this increased ROS level damages the mitochondria and results in RGC apoptosis, coupled with enhanced vascular permeability and retinal membrane leakage, leading to BRB breakdown and DR [6]. These biochemical alterations that provoke the apoptosis of cells due to mitochondrial damage are modulated by actuation of apoptosis supporting Bcl-2 proteins, enhancing oxidative stress, launching the caspase pathway, reduction of mitochondrial membrane potential (ΔYm) (MMP), and alterations in the cytochrome c distribution [7]. Altogether, restricting the oxidative damage due to hyperglycemia, and resulting RGC apoptosis, would prove an effective approach to prevent and treat DR.

Correspondence: Ming Zhou, Department of Ophthalmology, Affiliated Zhongshan Hospital of Dalian University, Dalian, China, e-mail: dr.mingzhou@hotmail.com
Received: 15.11.2021, Accepted: 01.03.2022

Scopoletin (SPT), a phenolic coumarin belonging to the family of phytoalexins, has been isolated from several plants including *Morinda citrifolia*, *Tetrapleura tetraptera* and *Polygala sabulosa.* SPT has been known to possess anti-oxidant and anti-inflammatory activity, and has apoptotic and autophagic potential [8]. The antioxidant activity of SPT has been found to be due to suppression of lipid peroxidation, and enhancing the activity of anti-oxidants, catalase and superoxide dismutase [9]. SPT has been established to exhibit potential autophagy mediated anti-aging activity via p53 modulation in lung fibroblasts of humans [10]. The expression of transcription factors Nrf2 and pFoxO1 has been found to be elevated due to SPT. In a rat model of rheumatoid arthritis, SPT resulted in apoptosis of fibroblast-like synoviocytes via the mitochondrial-dependent cascade by NF-kB inhibition and caspase-3 activation [11]. Also, investigations revealed that the anti-arthritic activity of SPT is mediated by anti-angiogenic variations and enhancement of angiogenic inducers such as IL-6, VEGF and FGF-2, which are known angiogenic inducers [12]. SPT has been reported to exert anti-depressant activity in experimental animals via modulation of serotonergic (5-HT2A/2C receptors), noradrenergic (α1- and α2-adrenoceptor) and dopaminergic (D1 and D2 receptors) systems [13]. SPT exhibits potential activity against diabetes mellitus via reactivation of insulin-triggered Akt/PKB phosphorylation in hepatocytes resistant to insulin, and further by permitting the PPARγ2 expression in adipocytes [14]. Also, SPT attenuates hyperglycemia and hepatic stenosis in diabetic mice exposed to a high fat diet, by reduction in the expression of gene and protein activity linked with biosynthesis of hepatic lipid. In the same experimental model, SPT suppressed the inflammation via modulation of the TLR4-MyD88-NF-κB signaling cascade [15].

Reports published earlier indicated that SPT markedly increased the uptake of glucose, which is linked with enhanced activity of PM-GLUT4 in 3T3-L1 adipocytes. The elevated PM-GLUT4 expression further stimulated PI3K and Akt activity, thereby resulting in increased intracellular uptake of glucose. Increased phosphorylation of AMPK coupled with increased PM-GLUT4 expression occurs due to SPT pre-conditioning in an animal model of diabetes [16]. Altogether, the findings suggest that SPT could induce potential activity against diabetic steatosis and inflammation in streptozotocin-induced diabetic mice. Administration of SPT has also been reported to impede the progression of cataract induced in a rat model by dietary galactose. The galactose induced swelling of lens fiber and the membrane distortion was found to be reversed with SPT administration [17]. Overall, the protective activity of SPT against sugar cataract was reported to be attributed to the suppression of aldose reductase activity and the oxidative stress in a rat model. On the basis of several investigations reported, SPT is an established pharmacologically active compound for diabetes mellitus and its related disorders, and other ailments. Hence it will be worth exploring whether SPT could exhibit protective effects on the retinal complications induced by apoptosis and oxidative stress associated with hyperglycemia.

However, the effect of SPT in the improvement of mitochondrial dysfunction and RGC apoptosis, due to increased glucose levels, has not been elucidated before. To investigate the effects of high glucose on the diabetes associated pathophysiological conditions, the commonly used model involves exposure to increased glucose levels *in vitro*. Hence, for the present investigation, we explored the protective effects of SPT on the retinal cells affected during diabetes mellitus. An *in vitro* RGC-5 model was developed to mimic the DR, under increased glucose concentrations, and examine its effect on the development of oxidative stress, apoptosis and loss of mitochondrial functionality.

Material and methods

Cell culture

The retinal ganglion cell culture RGC-5 has been established as a representative ganglion cell marker, and the cells behave as ganglion cells in an *in vitro* culture. The RGC-5 cell line was procured from American Type Culture Collection (ATCC, Manassas, VA, USA), and was cultured in Dulbecco's modified Eagle medium (DMEM – L-glutamine, 110 mg/l sodium bicarbonate and 1 g/l D-glucose) (Life Technologies, Carlsbad, CA, USA) blended with 10% fetal bovine serum (FBS) (Sigma-Aldrich, St. Louis, MO, USA), and penicillin-streptomycin (100 U/ml and 100 g/ml) (Sigma-Aldrich, St. Louis, MO, USA) respectively in a humidified environment at 25°C in an incubator with 5% CO_2. Under these conditions, after 20 h the RGC-5 count was approximately doubled. On alternate days, the medium was replaced and the cells were added to fresh medium at a ratio of 1 : 8. The RGC-5 cells recovered after 15-20 fresh medium transfers were collected and employed for the present investigation.

Exposure of RGC-5 cells to high-glucose concentration

The RGC-5 cells (2×10^6 cells/well) were allowed to grow in 12-well plates. After achieving uniformity of the cell growth in all the wells, the cell cultures were dissociated using trypsin (0.05% w/v) (Sigma-Aldrich, St. Louis, MO, USA) solution in pH 7.4 phosphate buffer saline (PBS). Before initiating the experimentation involving exposure of RGF-5 to high glucose exposure, the cells were kept for 2 h in culture containing 1% FBS. The cells were then subjected to variable concentrations of SPT (purity ≥ 99%; Cat. No. S2500; Sigma-Aldrich) – 0, 62.5, 125, 250, and 500 mM for 6 h. Variable concentrations of SPT were selected based on a previous report involving angiogenesis mediated investigation on human ECV304 cells,

but no earlier investigations reporting exposure of RGCs to SPT are documented [18]. The cells were then exposed for 48 h to 5.5 mmol/l as normal or 33.3 mmol/l as high concentration values of D-glucose. The SPT stock solution (10 mg/ml) was prepared in dimethyl sulfoxide (DMSO) (purity ≥ 99%; Cat. No. W387520; Sigma-Aldrich) and appropriate dilutions were made in the culture medium and then used in the investigation. Pure DMSO was utilized as a vehicle control in the experimental procedures. Three wells from each experimental group were quantified for viability of cells, ROS, oxidative and apoptotic markers in a replicate of five observations independently.

Estimation of cell viability

The RGC-5 cells were subjected to normal and high glucose concentrations with and without SPT, and the cell viability was estimated by MTT assay (Sigma-Aldrich). Approximately 1×10^4 cells dispersed in 100 ml of culture medium together with 10 ml of MTT solution were incubated for 3 h. Further to this, a detergent solution was added to break the cells and solubilize the colored crystals. The resulting absorbance was quantified using a microplate reader (Bio-Rad Laboratories, USA) at 490 nm. The viability of cells measured in control medium was considered as 100%, and accordingly the values in other experimental wells was measured. The cell viability was analyzed in three wells for each experimental group and was replicated five times.

Quantification of intracellular ROS

The intracellular production of ROS was estimated by treatment with a non-fluorescent compound, 2′,7′-dichlorodihydrouorescein diacetate (DCFDA), that undergoes oxidation in presence of ROS and gets converted to a fluorescent moiety, dichlorouorescin (DCF) [19]. A commercially available ROS detection kit (Abcam, Cambridge, MA, USA) was used according to the directions enclosed by the kit provider. Briefly, the RCF-5 culture (8×10^6 cells/ml) was diluted with PBS solution (pH 7.4) to a 2 ml volume. Further, 1 ml of DCFDA (100 ml; 10 mmol/l concentration) was added and subjected to incubation for half an hour at 37°C, followed by cleansing twice with PBS solution, and solubilizing in an aqueous solution of Triton-X100 (1% v/v). Finally, the cells were visualized under a fluorescence microplate reader (BioTek Instruments, Winooski, VT) and the fluorescence positive cell count was determined at 488 nm extinction wavelength and 535 nm emission wavelength.

Determination of protein carbonyl content and lipid peroxidation

The protein carbonyl content was estimated in the cell lysates using a commercially available protein carbonyl estimation kit (#ab126287; Abcam) by following the vendor's instructions. The quantification was performed on the basis of hydrazone generated by reacting the proteins with Brady's reagent, and determining the optical density at 370 nm wavelength. The protein carbonyl level was computed using the coefficient of absorption value 22,000/M/cm, and the findings were recorded as mmol/mg protein. The concentration of protein was estimated by employing the protein assay kit (Bio-Rad Laboratories Inc., CA, USA), by following the instructions provided with the kit. Peroxidation of lipid was investigated by quantifying the cellular malondialdehyde (MDA) in the lysates with the help of a lipid peroxidation assay kit (Abcam) following the directions provided by the manufacturer. The procedure included addition of 1 mmol/l of EDTA (Sigma-Aldrich) to 0.5 ml of cell homogenate (6×10^6 cells/ml) followed by mixing with 1 ml of cold thiobarbituric acid (TBA) (15% w/v) for coagulating the proteins. The collected supernatant was allowed to react in 1 ml (0.5% w/v) of TBA in a hot water bath for 15-20 min. The optical density of the cooled blend was then recorded at 535 nm wavelength, and the derivate generated by TBA was quantified considering MDA as a reference. The findings were recorded as mmol TBA generated derivative per mg of protein.

Estimation of antioxidative markers

The RGC-5 cells (2×10^6 cells/well) were cultured in plates with 6 wells. The levels of the anti-oxidant markers, namely, glutathione (GSH), glutathione peroxidase (GPx), catalase (CAT), and superoxide dismutase (SOD), were estimated following the instructions provided by the supplier.

The intracellular GSH level was quantified by employing the glutathione colorimetric estimation kit (BioVision Inc.) according to the enclosed guidelines. For estimation of intracellular GSH levels, the experimental cells were initially cleansed and devoid of protein content by treating with 2-hydroxy-5-sulfobenzoic acid (5% w/v) solution. The presence of GSH was quantified based on its reduction reaction with 6,6′-dinitro-3,3′-dithiodibenzoic acid resulting in 2-nitro-5-thiobenzoic acid (TNB) formation. Further TNB levels can be estimated by colorimetry at 412 nm, and the calculated GSH levels are represented in nmol/mg protein.

The GPx activity was quantified colorimetrically using a detection kit (BioVision Inc.) referring to the enclosed guidelines. The GPx catalyzes conversion of GSH to its oxidized derivative, which is then recycled back to form GSH with the help of GSH reductase and NADPH. Briefly the cell lysates were treated with GPx assay buffer containing a mixture of 50 mmol/l Tris HCl and 0.5 mmol/l EDTA, and the protocol provided with the kit was followed. At 340 nm the extent of NADPH oxidation by hydrogen peroxide was measured and the GPx expression was recorded in unit/mg protein.

The intracellular CAT activity in the experimental cells was estimated by employing a commercially available assay kit (BioVision Inc.). The estimation involves reaction

between methanol and CAT in the presence of hydrogen peroxide, followed by colorimetric determination of the generated formaldehyde at 540 nm wavelength using the chromogen 4-amino-5-hydrazino-1,2,4-triazole-3-thiol (Sigma-Aldrich, St. Louis, MO, USA). The activity of CAT was represented as unit/mg protein.

The SOD level was determined by employing a colorimetric detection kit (BioVision Inc.). A water-soluble dye, iodonitrotetrazolium chloride sodium salt, that undergoes reduction in the presence of the reactive superoxide O_2^- ion, of which the absorbance was determined at wavelength 450 nm, was employed in the present investigation. The rate and extent with which SOD suppresses the xanthine oxidase activity were determined in terms of SOD required for inhibiting by half the activity of xanthine oxidase/min/mg protein.

Determination of MMP (ΔYm)

The MMP (ΔYm) of RGC-5 cells was estimated with a commercially available detection kit involving 5,5′, 6,6′-tetrachloro-1,1′,3,3′-tetraethyl-imidacarbocyanineiodide (JC-1) (Invitrogen). Initially 1×10^4 cells were incubated in 16-well plates together with the JC-1 reagent (20 µmol/l) in the medium and incubated for 25 min at 37°C, followed by washing with cold PBS buffer (pH 7.4). Finally, fluorescence was measured using a spectrophotometer (F-2500; Hitachi), and the MMP (ΔYm) value was computed as the ratio of the intensity of red to green color fluorescence.

Determination of cytochrome c release

The cytosolic and mitochondrial portions were separated from the RGC-5 cells using a commercially available kit for fractionating mitochondria (#MIT1000, Sigma Aldrich) following the instructions enclosed with the kit. Initially, the experimental cells (8×10^6 cells/ml) were centrifuged for 5 min at 800 × g followed by resuspending the collected pellet with cold cytosolic buffer and subjecting to incubation for 15 min at 4°C. The homogenized cells were centrifuged twice at 800 × g for 20 min and the homogenate was collected. The supernatant was subjected to further centrifugation at 10,000 × g for 20 min, to result in sedimentation of mitochondria. The proteins were extracted from the mitochondrial fraction by inducing breakdown using the mitochondrial buffer and incubation for 15 min at 4°C. Consecutively, for collecting the cytosolic fraction, the supernatant was centrifuged at 16,000 × g for 30 min. The Bradford assay for employed for estimating the protein content. The cytochrome c levels in the mitochondrial and cytosolic fractions were estimated using an ELISA kit (Abcam), and following the instructions provided by the vendor.

Immunochemical analysis

The RGC-5 cells (8×10^6 cells/ml) were lysed and the protein fractions were collected from cytosolic and mitochondrial portions by following the manufacturer's instructions provided with the kit (#MIT1000, Sigma Aldrich). Following the procedure, the RGC-5 cells were subjected to 10 min of cryocentrifugation (800 × g), and further homogenized in the cold. The homogenates were then centrifuged at 800 × g for 15 min in the cold, and the resulting buoyant layer was centrifuged again for 20 min 10,000 × g at 4°C for collection of the cytosolic (supernatant) fraction, and the mitochondrial (sediment) fraction. The resulting proteins were estimated using the Bradford assay kit (Bio-Rad Laboratories), and further subjected to Western blot analysis using electrophoresis. The proteins were fractionalized by sodium dodecyl sulfate-polyacrylamide (10%) gel electrophoresis and transferred to polyvinylidene difluoride membranes. The membranes were further incubated for 3 hours at 37°C with a blend of 5% skimmed milk in Tris-buffered saline Tween (TBST) solution. Further, the membranes were incubated for 12 hours at 4°C along with primary antibodies against cytochrome c (#4272), cleaved caspase-3 (#9661), cleaved caspase-9 (#9501), Bcl-2 (#15071), Bax (#89477), JNK (#3708), p-JNK (#9255), p38 (#9212), and p-p38 (Thr180/Tyr182) (#9211) (Cell Signaling Technology). β-actin (#4967; Cell Signaling Technology), a reference standard, was employed to consider the presumed admixing of the mitochondrial fraction with cytosolic proteins. For analyzing the mitochondrial fraction, the standard used was primary antibody for cytochrome c oxidase subunit IV (COX IV) (#4850; Cell Signaling Technology). After completion of the incubation, the membranes were rinsed three times with TBST and again incubated for an hour with horseradish peroxidase-conjugated antibodies at room temperature. Thereafter, again the membranes were rinsed three times with TBST, and the resulting optical densities were imaged using chemiluminescence (Amersham Biosciences, UK), following the instructions provided by the manufacturer. The band densities were quantified using analyzing software (Quantity One 1-D; Bio-Rad, Hercules, CA), and recorded as the β-actin or COX IV ratio.

The average value for samples collected from the control group treated with normal glucose concentration on a densitometric scale was considered as unity (1.0), and the values obtained from experimental samples were calculated relative to this value. All the observations were recorded three times and individual experimental recording was performed five times.

Statistical analysis

The observations recorded were represented as a mean value ± standard deviation (SD). The statistical operations, and the resulting graphs were plotted using the SigmaPlot 12 software package (Systat Software Inc., USA). One-way analysis of variance (ANOVA) was executed as part of the statistical analysis. Dunnett's test for post-hoc variation was performed for the determination of possible sig-

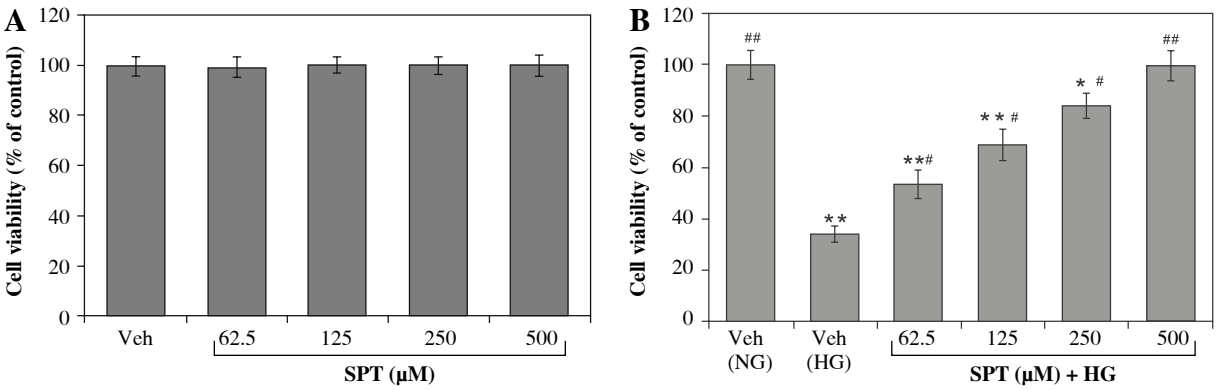

Fig. 1. RGC-5 cell viability is unaffected by scopoletin (SPT), and under high glucose concentration, SPT exhibits no cytotoxicity. The RGC-5 cells were cultured with normal (NG) or high glucose (HG) plus hesperidin at concentrations of 62.5, 125, 250 and 500 mM for 48 h. **A**) Effects of SPT treatments on cell viability of RGC-5 cells cultured with normal glucose concentration; **B**) Effects of treatments on cell viability in RGC-5 cells cultured with high glucose concentration. The cell viability was quantified by MTT. The results are presented as the mean ± standard deviation (SD) ($n = 5$), each of which was performed in triplicate. *$p < 0.05$ and **$p < 0.01$ when compared with the normal-glucose vehicle (Veh)-treated group. $^{\#}p < 0.05$ and $^{\#\#}p < 0.01$ when compared with the high-glucose vehicle-treated group

nificance among the resulting values. A p-value less than 0.05 was documented as statistically significant.

Results

Influence of SPT on high-glucose triggered RGC-5 cell death

The cultured RGC-5 cells incubated with normal glucose concentration for 48 hours, alone and with variable concentrations of SPT (62.5, 125, 250, and 500 mM) for 6 hours, indicated almost 100% viability of cells (no cytotoxicity) (Fig. 1A). Exposure of RGC-5 cells to high glucose concentration indicated 34.12% cell viability, whereas SPT treatment revealed the cell viability of 99.14% (at 500 mM) in the cell population exposed to high glucose concentration (Fig. 1B).

Influence of SPT on intracellular ROS, protein carbonyl content, lipid peroxidation and antioxidative markers in RGC-5 cells exposed to high-glucose environment

In RGC-5 cells exposed to high glucose concentration, the ROS, MDA and protein carbonyl content was significantly higher relative to those exposed to the normal concentration of glucose, that is the vehicle treated group. However, RGC-5 cells preconditioned with SPT and exposed to high glucose concentration revealed marked downregulation of the intracellular protein carbonyl level and the content of ROS and MDA (Fig. 2A-C).

Exposure of RGC-5 cells to high glucose levels revealed significantly reduced activity of SOD, GPx, CAT and GSH when correlated with the vehicle treated group. The intracellular content of SOD, GPx, CAT and GSH was significantly normalized in RGC-5 cells in the presence of variable concentration of SPT. Treatment of RGC-5 cells with SPT significantly upregulated the SOD, GPx, CAT and GSH activity, compared to those unexposed to SPT (Fig. 2D-G).

Influence of SPT on MMP (ΔYm) and cytochrome c release in high-glucose environment exposed RGC-5

In RGC5 cells that were exposed to high glucose concentration, the MMP (ΔYm) was lowered in comparison to that observed in RGC-5 cells subjected to normal glucose content. Further, the RGC-5 cells treated with SPT under a high-glucose environment revealed an increased value of MMP (ΔYm) in accordance with its increasing concentration (Fig. 3A).

Subsequently, when subjected to high glucose content, the RGC-5 cells revealed reduced mitochondrial and enhanced cytosolic content of cytochrome c. In the presence of an increasing SPT concentration, the movement of mitochondrial cytochrome c into the cytosol was significantly suppressed (Fig. 3B, C).

Influence of SPT on expression of high glucose induced apoptotic linked proteins in RGC-5 cells

Increased cleaved caspase-3 and cleaved capsase-9 expression was revealed in high glucose exposed RGC-5 cells, compared to that in the control vehicle group. The RGC-5 cells treated with increasing concentrations of SPT, and subjected to high-glucose concentration exposure, indicated marked reduction in the expression of cleaved caspase-3 and cleaved caspase-9 protein (Fig. 4A, B).

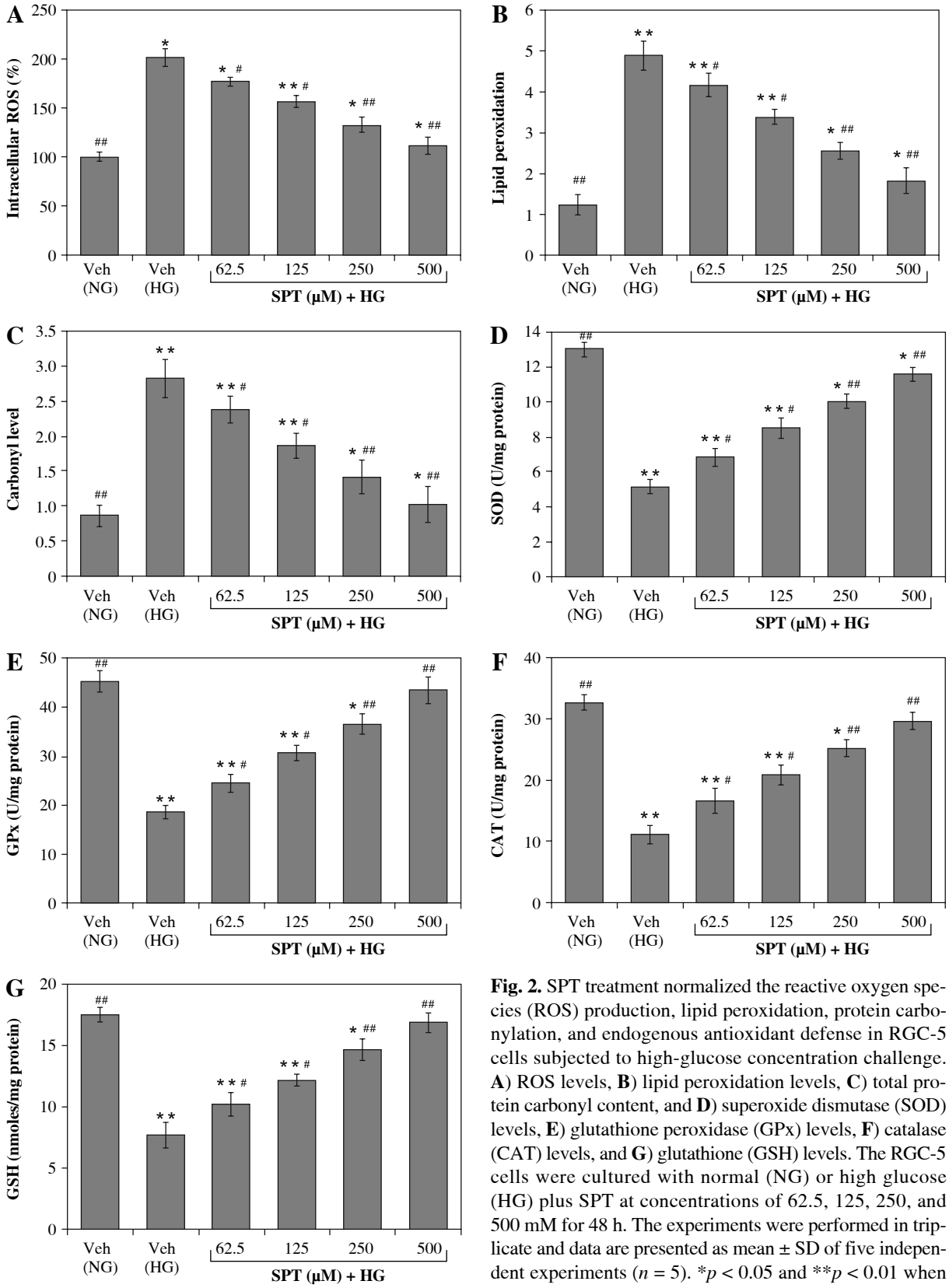

Fig. 2. SPT treatment normalized the reactive oxygen species (ROS) production, lipid peroxidation, protein carbonylation, and endogenous antioxidant defense in RGC-5 cells subjected to high-glucose concentration challenge. **A**) ROS levels, **B**) lipid peroxidation levels, **C**) total protein carbonyl content, and **D**) superoxide dismutase (SOD) levels, **E**) glutathione peroxidase (GPx) levels, **F**) catalase (CAT) levels, and **G**) glutathione (GSH) levels. The RGC-5 cells were cultured with normal (NG) or high glucose (HG) plus SPT at concentrations of 62.5, 125, 250, and 500 mM for 48 h. The experiments were performed in triplicate and data are presented as mean ± SD of five independent experiments ($n = 5$). *$p < 0.05$ and **$p < 0.01$ when compared with the normal-glucose vehicle (Veh)-treated group. $^{\#}p < 0.05$ and $^{\#\#}p < 0.01$ when compared with the high-glucose vehicle-treated group

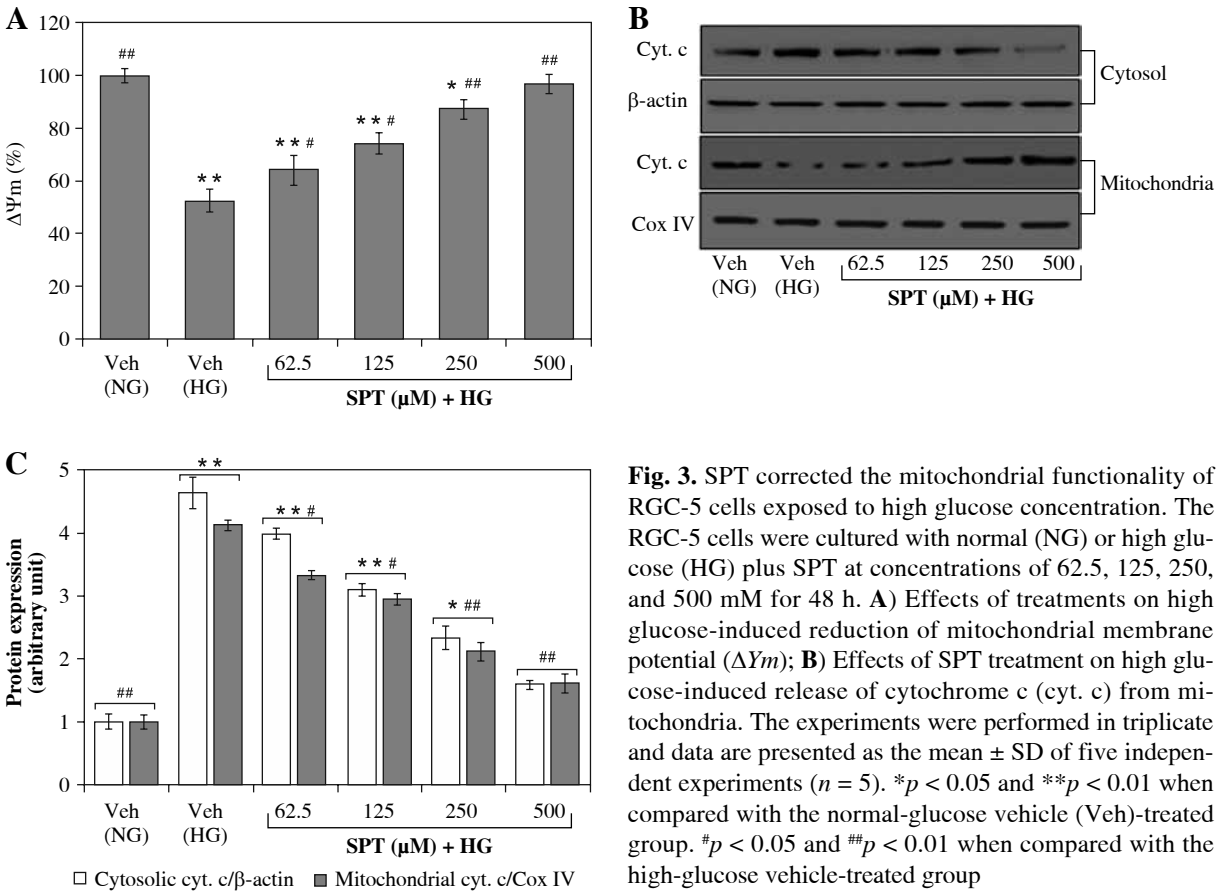

Fig. 3. SPT corrected the mitochondrial functionality of RGC-5 cells exposed to high glucose concentration. The RGC-5 cells were cultured with normal (NG) or high glucose (HG) plus SPT at concentrations of 62.5, 125, 250, and 500 mM for 48 h. **A**) Effects of treatments on high glucose-induced reduction of mitochondrial membrane potential (Δ*Ym*); **B**) Effects of SPT treatment on high glucose-induced release of cytochrome c (cyt. c) from mitochondria. The experiments were performed in triplicate and data are presented as the mean ± SD of five independent experiments ($n = 5$). $^{*}p < 0.05$ and $^{**}p < 0.01$ when compared with the normal-glucose vehicle (Veh)-treated group. $^{\#}p < 0.05$ and $^{\#\#}p < 0.01$ when compared with the high-glucose vehicle-treated group

The experimental RGC-5 cells in the high-glucose environment exhibited a significantly elevated ratio of Bax/Bcl-2 compared to the vehicle treated experimental cells. The Bax/Bcl-2 ratio was markedly normalized by incremental concentrations of SPT, compared to the SPT untreated RGC-5 cells (Fig. 4C, D).

Influence of SPT on the phosphorylation of JNK and p38 in RGC-5 cells exposed to high-glucose environment

The Western blot observation indicated that p-p38/p-38 and p-pJNK/pJNK proportions were significantly higher in RGC-5 cells subjected to high-glucose concentration exposure, in comparison to those exposed to the normal glucose concentration. Consecutively, treatment of high-glucose exposed RGC-5 cells with increasing SPT concentrations reduced the p-p38/p-38 and p-pJNK/pJNK ratio significantly, compared to the vehicle treated and high-glucose concentration experimental group (Fig. 5A-C).

Discussion

The investigation reported herewith demonstrates protective efficiency of SPT during oxidative stress triggered in RGC-5 cells under a high-glucose environment by regulation of MMP (Δ*Ym*), c-JNK and p38 MAPK, and suppressing the oxidative stress markers.

Several reports suggest critical involvement of oxidative stress in the development and progression of diabetic retinopathy [20, 21]. During elevated glucose levels various cell types have been reported to exhibit increased ROS generation. These increased ROS levels trigger perpetual intracellular reactions leading to large scale oxidation of lipids and proteins, thereby depleting their cellular content, which ultimately disturbs the normal cellular homeostasis, leading to cell death [22]. In this investigation, the oxidative stress resulting from the high glucose environment in RGC-5 cells was used as an experimental model to explore the *in vitro* protective effect of SPT. Earlier reports confirm an increase in the protein carbonyl and MDA levels in RGC-5 cells exposed high glucose content [23]. The enhanced MDA levels are a direct result of intracellular lipid breakdown due to elevated ROS levels during oxidative stress. Similarly, an increased carbonyl level is associated with protein damage owing to higher intracellular ROS generation [24]. Findings of the present investigation are in congruence with the earlier observations, indicating severe oxidative damage due to high glucose content. After SPT

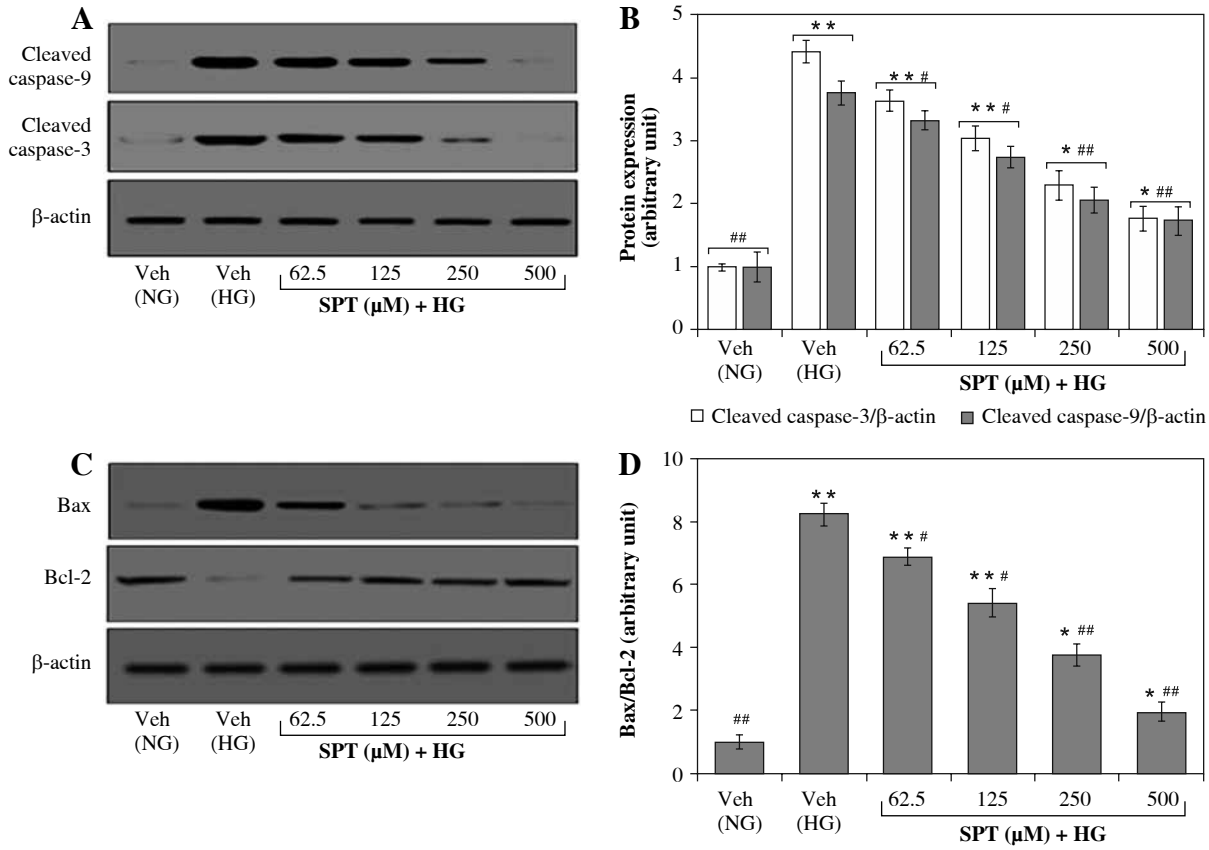

Fig. 4. SPT lowered the expression of cleaved caspase-3, cleaved capsase-9 protein and Bax/Bcl-2 ratio in RGC-5 cells exposed to high glucose concentration. The RGCs were cultured with normal (NG) or high glucose (HG) plus SPT at concentrations of 62.5, 125, 250, and 500 mM for 48 h. **A**) Protein bands of cleaved caspase-9 and cleaved caspase-3 in RGC-5 cells detected by Western blotting; **B**) Quantitative densitometric analysis of caspase-9 and cleaved caspase-3; **C**) Protein bands of Bax and Bcl-2 in RGC-5 cells detected by Western blotting; **D**) Changes of the ratios of Bax/Bcl-2 are displayed in the bottom panel. The results are presented as the mean ± SD of five independent experiments ($n = 5$), each of which was performed in triplicate. $^{*}p < 0.05$ and $^{**}p < 0.01$ when compared with the normal-glucose vehicle (Veh)-treated group. $^{\#}p < 0.05$ and $^{\#\#}p < 0.01$ when compared with the high-glucose vehicle-treated group

treatment, the levels of ROS, MDA and carbonyl content were markedly increased. The data support potential anti-oxidant activity of SPT in RGC-5 cells exposed to a high glucose environment.

Increased oxidative damage results in lowering of SOD, CAT and GPx in the event of high glucose exposure, which further impairs the anti-oxidative defense [25]. SOD lowers the formation of hydrogen peroxides by reducing breakdown to superoxide radicals. CAT influences the reduction of hydrogen peroxides and thereby shields against highly reactive hydroxyl moieties [26]. GPx activity is directly related to GSH, which is an important cofactor for several enzymes [27]. Reduction in the GSH activity cripples the cellular defense mechanisms towards intense oxidative stress that results during conditions such as diabetes. The present investigation revealed that SPT effectively imparted protection to the RGC-5 cells towards high glucose concentration mediated oxidative damage. Treatment with SPT resulted in control over the ROS levels by enhancing the anti-oxidant defense mechanism via enzymic and non-enzymic cascades.

Coumarins have been identified for their pro-apoptotic or anti-apoptotic activity, which depends on their effective concentration and the type of experimental cell model. In previous investigations, the apoptotic effect of SPT in numerous cancer cells has been reported [28]. Oxidative stress induced cell damage mediated by a high-glucose environment contributes to an extensive decrease in the MMP (ΔYm), and enhances cytosolic cytochrome c release, which eventually activates the cascade pathway and begins the cellular apoptotic cascade [29]. Our investigation revealed that in a high-glucose environment the MMP (ΔYm) of the RGC-5 cells was severely affected, which enhanced the cytochrome c release, thereby confirming the role of mitochondria in the apoptosis of RGC-5 cells in a high-glucose environment. The findings of our investi-

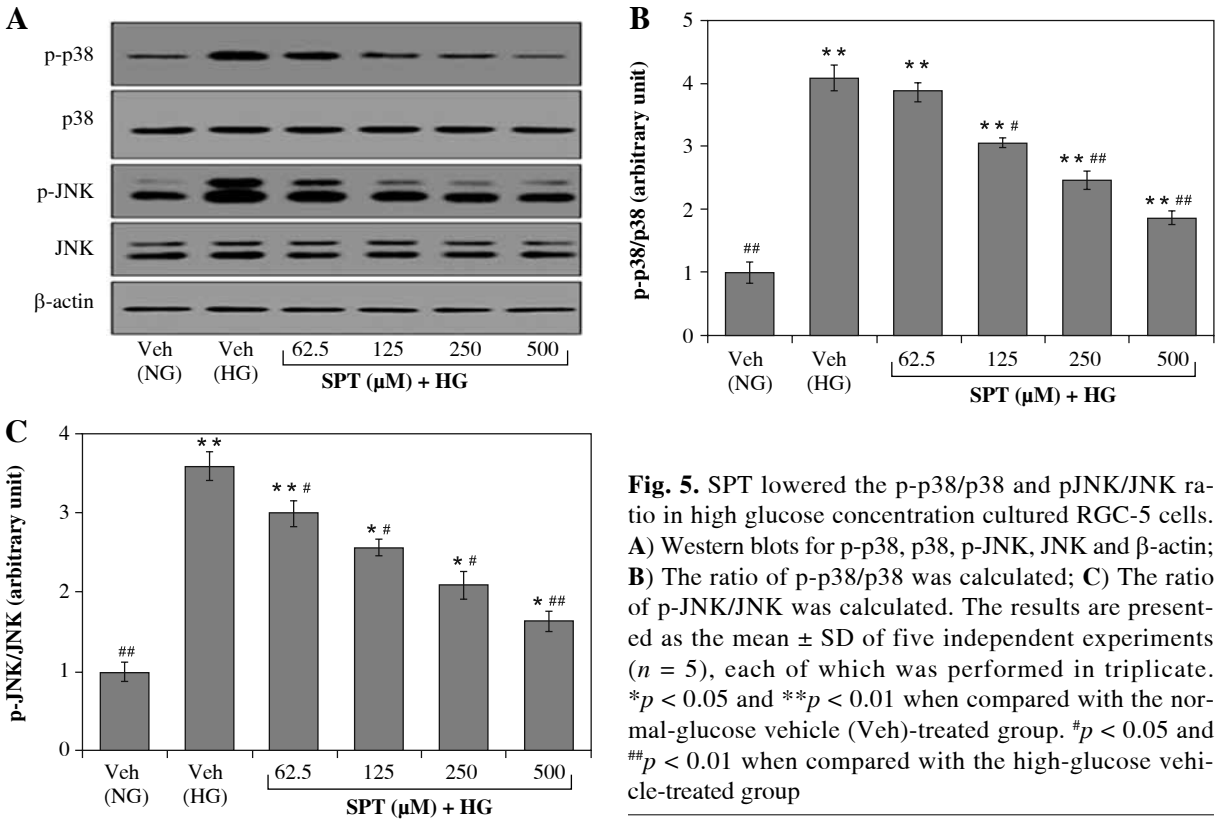

Fig. 5. SPT lowered the p-p38/p38 and pJNK/JNK ratio in high glucose concentration cultured RGC-5 cells. **A**) Western blots for p-p38, p38, p-JNK, JNK and β-actin; **B**) The ratio of p-p38/p38 was calculated; **C**) The ratio of p-JNK/JNK was calculated. The results are presented as the mean ± SD of five independent experiments (n = 5), each of which was performed in triplicate. $^{*}p < 0.05$ and $^{**}p < 0.01$ when compared with the normal-glucose vehicle (Veh)-treated group. $^{\#}p < 0.05$ and $^{\#\#}p < 0.01$ when compared with the high-glucose vehicle-treated group

gation indicated that treatment of RGC-5 cells with SPT and further exposure to high glucose concentration could revamp the mitochondrial functionality and further block the reduction of MMP (ΔYm) and eventually inhibit the cytosolic cytochrome c release. The RGC-5 cells did not exhibit marked toxicity after exposure to SPT. Under high glucose concentration, SPT increased the count of viable RGC-5 cells with maximum efficacy observed at 600 mM. Findings of the MTT assay established neuroprotective action of SPT towards RGC-5 cells exposed to high glucose induced mitochondrial damage.

In apoptosis mediated by mitochondrial damage, caspase-3 is activated by caspase-9, which in turn is triggered by the released cytochrome c [30]. Also, the Bcl-2 class proteins are known to critically regulate the MMP (ΔYm). The Bcl-2 proteins, known as anti-apoptotic proteins, reside in the outer mitochondrial membrane and are known to inhibit the membrane permeability, and the Bax proteins, recognized as pro-apoptotic proteins, are located in the mitochondrial membrane and enhance its permeability to release cytochrome c [31]. In RGC-5 cells exposed to increased glucose concentration, SPT exhibits an increase in Bax and a decrease in Bcl-2 activity, and lowers the caspase-9 and caspase-3 activity. Overall, SPT treatment lowers the caspase-9/3 and Bax/Bcl-2 activity ratio, in RGC-5 cells subjected to a high glucose environment. These findings clarify that SPT exposure defends the RGC-5 cells against apoptosis induced by a high-glucose environment via modulation of the mitochondrial mediated cascade.

A family of protein kinases, mitogen-activated protein kinases (MAPKs), have been well established to influence cell development and ROS-induced cell death. Under oxidative stress conditions, the antioxidants decrease the ROS levels and subsequently the activation of MAPK. The following classes of MAPK have been identified: c-Jun N-terminal kinases (JNKs), extracellular-signal regulated kinases 1 and 2 (ERK1/2), and p38 MAPK/stress-activated protein kinases. ERK1/2 have been known to be activated by mitogens and cell growth factors that modulate cellular growth and progression, whereas the JNK and p38 MAPK cascades have been established as pro-apoptotic cascades that are triggered during an event of hypoxic or oxidative stress [32]. Hence, for conferring protection against ROS exposure the regulation of the MAPK signaling cascade is crucial in cells. The results of our investigation revealed that SPT treatment markedly lowered the degree of phosphorylation of p38 and JNK in RGC-5 cells exposed to a high glucose concentration. These findings endorse the protection of RGC-5 cells subjected to a high glucose concentration by SPT treatment mediated by attenuation of p38 and JNK activity.

Overall, the investigation advocates the *in vitro* protective effect of SPT in RGC-5 cells against high-glucose

challenge by lowering the oxidative stress induced damage, modulation of the MMP, and reducing the p38 and JNK activation. Further, the investigation may be directed towards *in vivo* application in diabetic animals to confirm the activity of SPT, which may be further be extrapolated to a clinical level, which may present SPT as a novel molecule in the treatment of diabetic retinopathy.

The authors declare no conflict of interest.

References

1. Nentwich MM, Ulbig MW (2015): Diabetic retinopathy-ocular complications of diabetes mellitus. World J Diabetes 6: 489-499.
2. Stitt AW, Curtis TM, Chen M, et al. (2016): The progress in understanding and treatment of diabetic retinopathy. Prog Retin Eye Res 51: 156-186.
3. Cai J, Boulton M (2002): The pathogenesis of diabetic retinopathy: old concepts and new questions. Eye 16: 242-260.
4. Kern TS, Barber AJ (2008): Retinal ganglion cells in diabetes. J Physiol 586: 4401-4408.
5. Brownlee M (2005): The pathobiology of diabetic complications: A unifying mechanism. Diabetes 54: 1615-1625.
6. Feenstra DJ, Yego EC, Mohr S (2013): Modes of retinal cell death in diabetic retinopathy. J Clin Exp Ophthalmol 4: 298.
7. Luna-Vargas MP, Chipuk JE (2016): The deadly landscape of pro-apoptotic BCL-2 proteins in the outer mitochondrial membrane. FEBS J 283: 2676-2689.
8. Liu XL, Zhang L, Fu XL, et al. (2003): Effect of scopoletin on pc3 cell proliferation and apoptosis. Acta Pharmacol Sin 22: 929-933.
9. Shaw CY, Chen CH, Hsu CC, et al. (2003): Antioxidant properties of scopoletin isolated from Sinomonium acutum. Phytother Res 17: 823-825.
10. Nam H, Kim MM (2015): Scopoletin has a potential activity for anti-aging via autophagy in human lung fibroblasts. Phytomedicine 22: 362-368.
11. Li Y, Dai Y, Liu M, et al. (2009): Scopoletin induces apoptosis of fibroblast-like synoviocytes from adjuvant arthritis rats by a mitochondrial-dependent pathway. Drug Dev Res 70: 378-385.
12. Pan R, Gao XH, Lu D, et al. (2011): Prevention of FGF-2-induced angiogenesis by scopoletin, a coumarin compound isolated from Erycibe obtusifolia Benth, and its mechanism of action. Int Immunopharmacol 11: 2007-2016.
13. Capra JC, Cunha MP, Machado DG, et al. (2010): Antidepressant-like effect of scopoletin, a coumarin isolated from Polygala sabulosa (Polygalaceae) in mice: Evidence for the involvement of monoaminergic systems. Eur J Pharmacol 643: 232-238.
14. Zhang WY, Lee JJ, Kim Y, et al. (2010): Amelioration of insulin resistance by scopoletin in high-glucose-induced, insulin-resistant HepG2 cells. Horm Metab Res 42: 930-935.
15. Choi RY, Ham JR, Lee HI, et al. (2017): Scopoletin supplementation ameliorates steatosis and inflammation in diabetic mice. Phytother Res 31: 1795-1804.
16. Jang JH, Park JE, Han JS (2020): Scopoletin increases glucose uptake through activation of PI3K and AMPK signaling pathway and improves insulin sensitivity in 3T3-L1 cells. Nutr Res 74: 52-61.
17. Kim J, Kim C-S, Lee YM, et al. (2013): Scopoletin inhibits rat aldose reductase activity and cataractogenesis in galactose-fed rats. Evid Based Complement Alternat Med 2013: 787138.
18. Pan R, Dai Y, Yang J, et al. (2009): Anti-angiogenic potential of scopoletin is associated with the inhibition of ERK1/2 activation. Drug Dev Res 70: 214-219.
19. Rastogi RP, Singh P, Häder DP, et al. (2010): Detection of reactive oxygen species (ROS) by the oxidant-sensing probe 20,70-dichlorodihydrofluorescein diacetate in the cyanobacterium Anabaena variabilis PCC 7937. Biochem Biophys Res Commun 397: 603-607.
20. Ihnat MA, Thorpe JE, Kamat CD, et al. (2007): Reactive oxygen species mediate a cellular 'memory' of high glucose stress signalling. Diabetologia 50: 1523-1531.
21. Cao Y, Li X, Shi P, et al. (2014): Effects of L-carnitine on high glucose-induced oxidative stress in retinal ganglion cells. Pharmacology 94: 123-130.
22. Vakifahmetoglu-Norberg H, Ouchida AT, Norberg E (2017): The role of mitochondria in metabolism and cell death. Biochem Biophys Res Commun 482: 426-431.
23. Wang Y, Zhang H, Liu Y, et al. (2015): Erythropoietin (EPO) protects against high glucose-induced apoptosis in retinal ganglional cells. Cell Biochem Biophys 71: 749-755.
24. Mano J (2012): Reactive carbonyl species: Their production from lipid peroxides, action in environmental stress, and the detoxification mechanism. Plant Physiol Biochem 59: 90-97.
25. Matés JM, Sánchez-Jiménez F (1999): Antioxidant enzymes and their implications in pathophysiologic processes. Front Biosci 4: D339-D345.
26. Liedias F, Rangel B, Hansberg W (1998): Oxidation of catalase by singlet oxygen. J Biol Chem 273: 10630-10637.
27. Melov S (2002): Animal models of oxidative stress, aging and therapeutic antioxidant interventions. Int J Biochem Cell Biol 34: 1395-1400.
28. Seo EJ, Saeed M, Law BYK, et al. (2016): Pharmacogenomics of scopoletin in tumor cells. Molecules 21: 496-519.
29. Gupta S, Kass GE, Szegezdi E, et al. (2009): The mitochondrial death pathway: A promising therapeutic target in diseases. J Cell Mol Med 13: 1004-1033.
30. Luna-Vargas MP, Chipuk JE (2016): Physiological and pharmacological control of BAK, BAX, and beyond. Trends Cell Biol 26: 906-917.
31. Son Y, Kim S, Chung HT, et al. (2013): Reactive oxygen species in the activation of MAP kinases. Methods Enzymol 528: 27-48.
32. Kyaw M, Yoshizumi M, Tsuchiya K, et al. (2001): Antioxidants inhibit JNK and p38 MAPK activation but not ERK 1/2 activation by angiotensin II in rat aortic smooth muscle cells. Hypertens Res 24: 251-261.